Dear Editors and Referees:

Thank you very much for your review and comments concerning our manuscript entitled "Elevated 3D structures of $PM_{2.5}$ and impact of complex terrain-forcing circulations on heavy haze pollution over Sichuan Basin, China" [MS No.: acp-2020-1161]. We have revised the manuscript accordingly. All the revisions have been highlighted with Track Changes in the revised manuscript. In the following, we quoted each review question in the square brackets and added our response after each paragraph.

==

Response to Editor:

==

[1.Concerning the model configuration: It would be interesting to know how many vertical levels you used in the model above the boundary level, and what is your model top. Please add those information in the manuscript.]

Response 1: Thanks for your comments. we have revised the sentence in Sect. 2.3. "Therefore, 35 vertical layers from the ground to the model top at 100 hPa were set for the modeling experiments in this study on air pollution change with the 18 layers in the fine resolutions of 30–120 m vertically from the ground to 1km within the atmospheric boundary layer."

[2. Furthermore, you don't explain why you use MYJ as a boundary layer scheme. There are other schemes in WRF, such as MYNN, which might have a different turbulent diffusion coefficient and a different treatment of the PBL dynamics. Please add a reference that have used MYJ for a similar work in a complex terrain environment (e.g. in California or Colorado in the USA or over China).]

Response 2: Thank the referee for the suggestion. There are various planetary boundary layer schemes in WRF, including the nonlocal closure schemes (MRF, YSU and SH schemes) and local closure schemes (e.g., MY series schemes). Aims at the stable atmospheric stratification and weak turbulent mixing over the complex terrain, such as California (Lu et al., 2012), Jharkhand state of India (Madala et al., 2015) and Beijing-Tianjin-Hebei region in China (Bei et al., 2019), the MYJ produced better model performance. Following your suggestion, the explanation on the MYJ scheme has been revised in Sect. 2.3 as follows:

"The MYJ is a local closure scheme (Janjić, 1994), which is applicable to the atmospheric environment with stable atmospheric stratification for weak turbulent mixing (Jia and Zhang, 2020) and underlying complex terrain (Lu et al., 2012; Madala et al., 2015; Bei et al., 2019). Therefore, the MYJ was used as the planetary boundary layer parameterization scheme in the simulation."

Table 2. Setting of physical and chemistry schemes in the WRF-Chem simulations

Microphysics	Morrison 2-mom
Boundary layer	MYJ
Longwave radiation	RRTM
Shortwave radiation	RRTMG
Land surface	Noah
Cumulus convection	Grell 3D (none in D3)
Urban scheme	Single-layer
Chemistry	RADM2
Aerosol particles	MADE/SORGAM
Photolysis	Madronich (TUV)

References

Janjić, Z.: The step-mountain eta coordinate model: further developments of the convection, viscous sublayer, and turbulence closure schemes, Mon. Weather Rev., 122 (5), 927–945, https://doi.org/10.1175/1520-0493(1994)122<0927:TSMECM>2.0.CO;2, 1994.

Jia, W. and Zhang, X.: The role of the planetary boundary layer parameterization schemes on the meteorological and aerosol pollution simulations: A review, Atmos. Res., 239, 104890, https://doi.org/10.1016/j.atmosres.2020.104890, 2020.

Lu, W., Zhong, S., Charney, J., Bian, X. and Liu, S.: WRF simulation over complex terrain during a southern California wildfire event, J. Geophys. Res., 117(D5), https://doi.org/10.1029/2011JD017004, 2012.

Madala, S., Satyanarayana, A., Srinivas, C. and Kumar, M.: Mesoscale atmospheric flow-field simulations for air quality modeling over complex terrain region of Ranchi in eastern India using WRF, Atmos. Environ., 107, 315–328, https://doi.org/10.1016/j.atmosenv.2015.02.059, 2015.

Bei, N., Li, X., Tie, X., Zhao, L., Wu, J., Li, X., Liu, L., Shen. Z. and Li, G.: Impact of synoptic patterns and meteorological elements on the wintertime haze in the Beijing-Tianjin-Hebei region, China from 2013 to 2017. Sci. Total Environ., 704, 135210, https://doi.org/10.1016/j.scitotenv.2019.135210, 2019.

[3. Figure S1 and S2 are not discussed in the paper. Please add a comment on those figures in the main article.]

Response 3: Thanks for your comments. In the revised manuscript, we have accordingly modified in Sect. 3.1:

"First, we validated the WRF-Chem simulation performance by comparing with the meteorological and $PM_{2.5}$ observations in the SCB, especially with the intensive vertical soundings, for verifying the vertical structures of the simulated boundary layer (Fig. S1-S3)."

[4. Figure S3: please add the date and time information on top of each subplots.]

Response 4: Thanks for your suggestion, we have added the date and time information on each subplot in Figure S3 as follows:

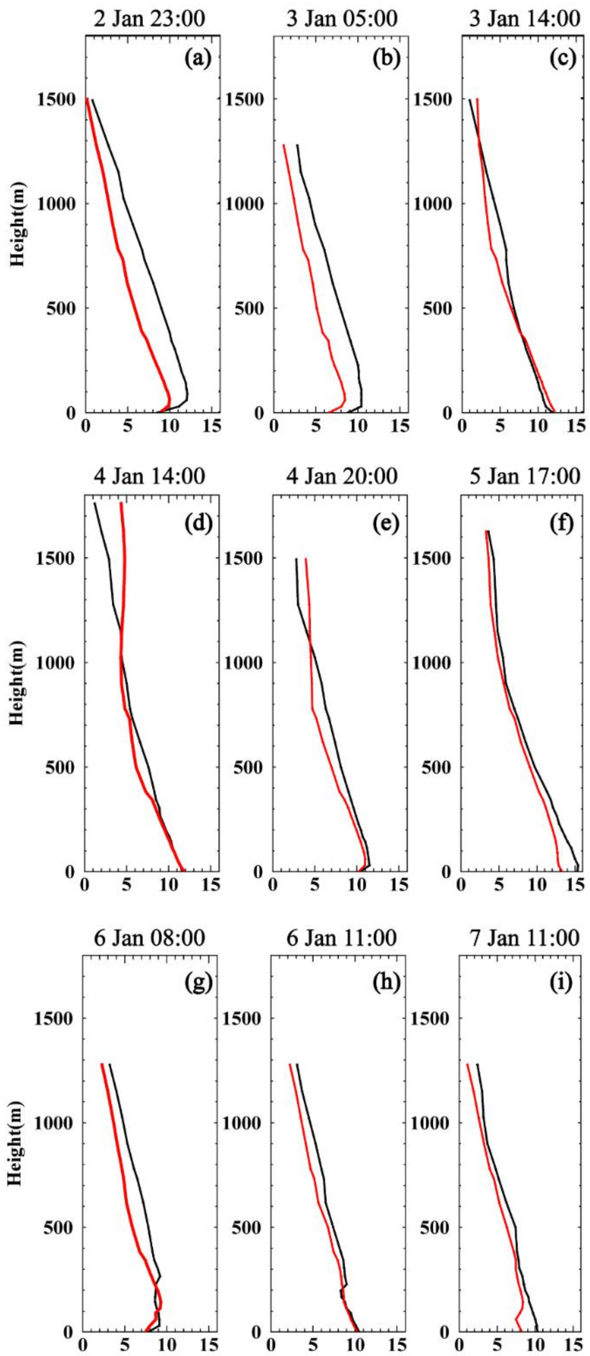

Figure S3. Comparisons of vertical profiles of air temperature between observation (black curves) and simulation (red curves).

[5. Table 3: add the units to T2, RH and WS10, and define in the caption what it refers to]

Response 5: We have modified the caption of Table 3 and added the responding units.

Table 3. Statistical metrics of comparisons between simulated (Sim.) and observed (Obs.) 2-m air temperature (T2), surface relative humidity (RH) and 10-m wind speed (WS10) with the correlation coefficient (R), mean bias(MB), mean error (ME) and root mean squared error (RMSE) during air pollution process over 2–7 January 2017.

	Obs.	Sim.	R	MB	ME	RMSE
T2	9.9℃	9.2℃	0.78**	−0.7	1.7	2.1
RH	85.1 %	77.7 %	0.67**	−7.4	11.2	13.4
WS10	1.2 m s^{-1}	1.5 m s^{-1}	0.41*	0.3	0.8	1.1

Note: MB, ME, RMSE were calculated as following: $MB = \frac{1}{N}\sum_{i=1}^{N}(M_i - O_i)$; $ME = \frac{1}{N}\sum_{i=1}^{N}|M_i - O_i|$; $RMSE = \sqrt{\frac{1}{N}\sum_{i=1}^{N}(M_i - O_i)^2}$; (M and O represented the results from simulation and observation). The ** and * respectively indicated the correlation coefficients R passing the 99% and 95% significant test.

==

Response to Referee

==

[1. Meteorological conditions

Given the synoptic conditions, I still do not understand the reason for the increase of northeasterly winds during the dissipation stage. A more detailed description of these mechanisms would be in my opinion beneficial for the reader not expert of the meteorology of this region.]

Response 1: The description of synoptic mechanisms was added in the revised Sect. 2.4 as follows:

"Under the typical Asian monsoon climate in January over the SCB, the change of synoptic conditions during the haze event over the SCB were characterized by the cold air invasion driven by near-surface northeasterly winds with the vertical configuration of trough development and movement in the mid-latitude westerlies at 700 hPa (Figs. 3 and 7). A 700 hPa trough in the mid-latitude westerlies moved eastward from the eastern edge of the TP to the western SCB margin during P1 (Fig. 3a), the trough of low pressure evolved at 700 hPa during P2 (Fig. 3b), and the 700-hPa trough and the low-pressure system disappeared in P3 over the SCB (Fig. 3c). Meteorologically, the direction and intensity of cold air invasion with near-surface northeasterly winds are steered by the development and movement of the westerly trough in the mid-troposphere (Fig. 3c). The 700-hPa trough approached, developed and disappeared in P1, P2 and P3 of the haze pollution event over the SCB (Fig. 3), which is associated with the increase of northeasterly winds for the cold air invasion to the SCB region during the dissipation stage. The changes in atmospheric circulations in the three stages reflected the meteorological modulation of heavy haze development over the SCB in association with the effect of TP topography on the westerlies."

[*2. Model set-up*

Some choices in the model set-up are still not clear. The explanation of the choice of the 1:4 grid ratio is not clear. Why the presence of complex terrain should be the explanation? Moreover, it is not clear on which basis the Authors decided to cut half the turbulent diffusion coefficient. Did You run some sensitivity tests?]

Response 2: The description of the model set-up and the choice of the 1:4 grid ratio have been modified as follows, and the revised Table 2 is also listed. We did the sensitivity tests with changing turbulent diffusion coefficient, and the test with cutting half the turbulent diffusion coefficient was validated with the most reasonable simulation of air pollutants over the SCB.

"The MYJ is a local closure scheme (Janjić, 1994), which is applicable to the atmospheric environment with stable stratification for weak turbulent mixing (Jia and Zhang, 2020) and underlying complex terrain (Lu et al., 2012; Madala et al., 2015;

Bei et al., 2019). Therefore, The MYJ was used as the planetary boundary layer parameterization scheme in the simulation. The detailed physical and chemistry schemes for the WRF-Chem simulation are listed in Table 2, involving the Morrison 2 microphysics (Morrison et al., 2009), the RRTM longwave radiation (Mlawer et al., 2000), the RRTMG shortwave radiation (Iacono et al., 2008), Noah land surface model (Tewari et al., 2004) and the Grell 3D cumulus (Grell and Devenyi, 2002)."

Table 2. Setting of physical and chemistry schemes in the WRF-Chem simulations

Microphysics	Morrison 2-mom
Boundary layer	MYJ
Longwave radiation	RRTM
Shortwave radiation	RRTMG
Land surface	Noah
Cumulus convection	Grell 3D (none in D3)
Urban scheme	Single-layer
Chemistry	RADM2
Aerosol particles	MADE/SORGAM
Photolysis	Madronich (TUV)

"Considering the sharp drop of topography between the SCB and surrounding plateaus and mountains with the terrain influence on westerlies and atmospheric circulations, we adopted the 1:4 grid ratio for simulation experiments. Although an even nested ratio, which is not recommended, may result in interpolation errors at the nested-domain boundary owing to the nature of Arakawa C-grid staggering, the 1:4 grid ratio available in the WRF framework was reasonably applied in previous simulation studies (Tie et al., 2010; Rai et al., 2019)."

"The weakened vertical diffusion capacity is conducive to the accumulation of air pollutants (Ren et al., 2019) and in the formation of severe haze pollution with the explosive growth of $PM_{2.5}$ (Zhong et al., 2018). Approximately 80 % reduction in turbulent diffusion coefficient provides a more accurate prediction of $PM_{2.5}$ over the NCP (Wang et al., 2018). High $PM_{2.5}$ levels in the atmosphere could significantly reduce the near-ground solar radiation, resulting in decreasing vertical turbulent diffusion in the boundary layer (Wang et al., 2019), which could be incompletely considered in the meteorological reanalysis data driving the WRF-Chem simulation. In this study, we found that a 50 % decrease of the turbulent diffusion coefficient in the SCB could greatly improve the deviation of $PM_{2.5}$ simulations in the extremely stable atmosphere through the sensitivity tests. Hence, the turbulent diffusion coefficient was cut halfway for the simulation of the 3D structures of $PM_{2.5}$, during the heavy air pollution event over the SCB region."

References

Lu, W., Zhong, S., Charney, J., Bian, X. and Liu, S.: WRF simulation over complex terrain during a southern California wildfire event, J. Geophys. Res., 117(D5), https://doi.org/10.1029/2011JD017004, 2012.

Madala, S., Satyanarayana, A., Srinivas, C. and Kumar, M.: Mesoscale atmospheric flow-field simulations for air quality modeling over complex terrain region of Ranchi in eastern India using WRF, Atmos. Environ., 107, 315–328, https://doi.org/10.1016/j.atmosenv.2015.02.059, 2015.

Bei, N., Li, X., Tie, X., Zhao, L., Wu, J., Li, X., Liu, L., Shen. Z. and Li, G.: Impact of synoptic patterns and meteorological elements on the wintertime haze in the Beijing-Tianjin-Hebei region, China from 2013 to 2017. Sci. Total Environ., 704, 135210, https://doi.org/10.1016/j.scitotenv.2019.135210, 2019.

Janjić, Z.: The step-mountain eta coordinate model: further developments of the convection, viscous sublayer, and turbulence closure schemes, Mon. Weather Rev., 122 (5), 927–945, https://doi.org/10.1175/1520-0493(1994)122<0927:TSMECM>2.0.CO;2, 1994.

Jia, W. and Zhang, X.: The role of the planetary boundary layer parameterization schemes on the meteorological and aerosol pollution simulations: A review, Atmos. Res., 239, 104890, https://doi.org/10.1016/j.atmosres.2020.104890, 2020.

Morrison, H., Thompson, G. and Tatarskii, V.: Impact of cloud microphysics on the development of trailing stratiform precipitation in a simulated squall line: Comparison of one- and two-moment schemes, Mon. Weather Rev., 137(3), 991–1007. https://doi.org/10.1175/2008MWR2556.1, 2009.

Mlawer, E. J., Taubman, S. J., Brown, P. D., Iacono, M. J., and Clough, S. A.: Radiative transfer for inhomogeneous atmospheres: RRTM, a validated correlated-k model for the longwave, J. Geophys. Res., 102, 16663–16682, https://doi.org/10.1029/97JD00237, 1997.

Iacono, M., Delamere, J., Mlawer, E., Shephard, M., Clough, S. and Collins, W.: Radiative forcing by long - lived greenhouse gases: Calculations with the AER radiative transfer models, J. Geophys. Res., 113, D13103, https://doi.org/10.1029/2008JD009944, 2008.

Tewari, M., Chen, F., Wang, W., Dudhia, J., LeMone, M. A., Mitchell, K., Ek, M., Gayno, G., Wegiel, J., and Cuenca, R. H.: Implementation and verification of the unified NOAH land surface model in the WRF model, in 20th conference on weather analysis and forecasting/16th conference on numerical weather prediction, 14 January 2004, Seattle, WA, USA, 11–15, 2004.

Grell, G. A. and Devenyi, D.: A generalized approach to parameterizing convection combining ensemble and data assimilation techniques, Geophys. Res. Lett., 29, 1693, https://doi.org/10.1029/2002GL015311, 2002.

Tie, X., Brasseur, G., and Ying, Z.: Impact of model resolution on chemical ozone formation in Mexico City: application of the WRF-Chem model, Atmos. Chem. Phys., 10, 8983–8995, https://doi.org/10.5194/acp-10-8983-2010, 2010.

Rai, R., Berg, L., Kosović, B., Sue, E., Jeffrey, D., Brandon, L., and Caroline, D.: Evaluation of the impact of horizontal grid spacing in terra incognita on coupled mesoscale–microscale simulations using the WRF framework. Mon. Weather Rev., 147(3): 1007-1027, https://doi.org/10.1175/MWR-D-18-0282.1, 2019.

[3. Results

Section 3.3 should be re-organized since it is not clear and many concepts are repeated at different points with different words.Moreover, from Fig. 8 I cannot see the differences between the different phases highlighted by the Authors at lines 269-275 (PM2.5 elevated to the free atmosphere in clean environment and dissipation periods and pressed down in formation and maintenance periods). For example, I can see upward arrows in Fig. 8c, where the Authors indicate the downward branch of the vortex. The most significant difference that I can see in Figure 8 is the stronger low-level wind in Fig. 8d (but I cannot understand the cause of this wind, see above)]

Response 3: Thanks for the referee's suggestions. According to the suggestions, 1) we have revised the original lines 269-275 with "Similarly, $PM_{2.5}$ elevated to the free atmosphere in a clean environment and dissipation periods and pressed down in formation and maintenance periods", 2) we have modified the upward and downward arrows in the revised Fig. 8c, and 3) added the cause of the stronger low-level winds in Fig. 8d (please also see the response 1).

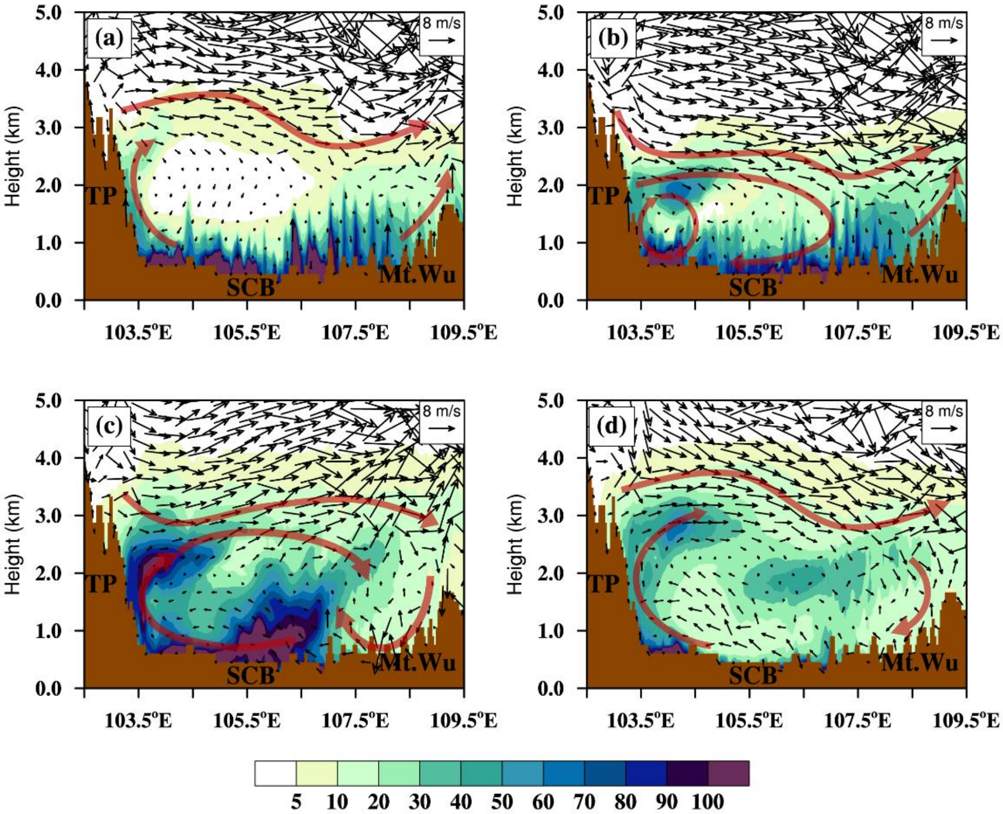

Figure 8. Height-longitude cross-sections of $PM_{2.5}$ concentrations (color contours: μg m^{-3}) and wind vectors along 30.67º N in the (a) clean environment at 12:00 a.m. on 2 January 2017 (b) heavy air pollution formation stage at 12:00 a.m. on 3 January 2017 (c) maintenance stage at 8:00 a.m.on 6 January 2017, and (d) dissipation stage at 8:00 a.m. on 7 January 2017. The brown arrows highlighted the major air flows (red arrows) associated with the terrain of TP, SCB and Mt. Wu (filled brown color).

In the revised manuscript, section 3.3 has been accordingly re-organized and modified with the above discussions as follows:

"The terrain effect of TP, the "world roof" on the mid-latitude westerlies could modulate haze pollution in the downstream region over China (Xu et al., 2016). The SCB is immediate to the east of the TP, with a large elevation drop exceeding 3000 m over a short horizontal distance. The unique terrain-forcing circulations generate asymmetries in meteorological and air pollutant distributions over the SCB (Zhang et al., 2019). Chengdu (site 1: 104.02° E; 30.67° N) which is a metropolis in SCB with high anthropogenic pollutant emissions and has the highest pollution levels in Southwest China (Ning et al., 2018b), situated on the far west side of the SCB, was selected to better understand the elevated 3D structures of $PM_{2.5}$. It is important to investigate how the urban surface high $PM_{2.5}$ levels evolved vertically in the atmosphere with the combination of high urban emissions and TP's terrain-forcing lifting over SCB.

The distributions of $PM_{2.5}$ and the atmospheric circulations in the vertical-meridional and vertical-zonal cross-sections over the SCB and surrounding areas, respectively, are shown in Figs. 8 and 9 for a clean environment, formation, maintenance, and dissipation periods of the heavy haze pollution episode. A remarkable feature in the vertical distributions of $PM_{2.5}$ was the unique hollows over the SCB region, between the two high $PM_{2.5}$ layers at the surface and heights of 1.5–3 km. Similarly, $PM_{2.5}$ elevated to the free atmosphere in a clean environment and dissipation periods and pressed down in formation and maintenance periods. The special phenomenon was developed by the interaction of atmospheric circulations in the free troposphere and topographic forcing in the boundary layer. In the atmospheric boundary layer, the leeside vortices often occur over the SCB owing to the effect of the large TP topography on the mid-latitude westerlies, which reinforces the vertical exchange of $PM_{2.5}$ concentrations (Zhang et al., 2019). Meanwhile, a strong temperature inversion appeared and acted as a lid covering $PM_{2.5}$ due to the trough of a low-pressure system (Ning et al., 2018a). In the current case, the variations of lee vortex circulation, working together with the basin near-surface flows, drove a 3D $PM_{2.5}$ transport and its temporal changes over the SCB (Figs. 8–9).

Driven by the near-surface northeasterly winds (Fig. 7), the high concentrations of near-ground $PM_{2.5}$ over the SCB were uplifted over the windward slopes of TP and YGP, respectively. Comparing the vertical structures of $PM_{2.5}$ and the circulations in different periods, the southwesterly wind prevailed at approximately 3 km height in the clean and dissipation stages (Figs. 8a, 8d, 9a, and 9d). It means that the elevated $PM_{2.5}$ transport process in the free troposphere is a general pattern with the plateau-basin configuration over the SCB. By contrast, the so-called lid with a southwesterly wind in vortex circulation was pressed down to 2 km over the SCB. The uphill airflows were restrained and overturned below 2.5 km (a.s.l.), forming a well-structured vertical sub-circulation over the SCB region (Figs. 8b, 8c, 9b and 9c). Governed by the vertical sub-circulations, the downward transport from the high $PM_{2.5}$ layers could replenish the surface $PM_{2.5}$ concentrations in the northwest SCB with the addition of near-surface accumulation and maintenance of air pollutants. The sink momentum of vertical sub-circulation was weakened and confined $PM_{2.5}$ exchange along with the eastern TP while the trough evolves into a low-pressure system (Figs. 3b, 8c and 9c). The cold air invasion with stronger near-surface northeasterly winds steered by the movement of a westerly trough in the mid-troposphere during the dissipation stage of $PM_{2.5}$ pollution (Figs. 3c, 8d and 9d). The haze pollution event over SCB integrally indicated the formation of elevated $PM_{2.5}$ structure and reconstruction of trans-boundary transport pattern of $PM_{2.5}$."

"The complex terrain-forcing circulations along the windward slopes of TP and YGP, accompanying the lowering of westerlies lid, drove a remarkable hollow of $PM_{2.5}$ sandwiched by a high $PM_{2.5}$ layer in the free troposphere and a highly polluted near-surface layer in northwest SCB. It was also noted that the high $PM_{2.5}$ concentrations over the SCB were transported to the downwind regions following westerlies by a special pathway above the atmospheric boundary layer."

[4. Page 6, line 160: the date of the end of the dissipation stage is wrong.]

Response 4: Thanks for your careful review. The concentrations of $PM_{2.5}$ pollution event indeed ended on 7 January 2017 and there is an error in our description here. We have corrected it accordingly in the manuscript.

[5. Figure 9: I think the caption is not correct.]

Response 5: The caption of Figure 9 has been modified as:

"Same as Fig. 8, but for height-latitude cross-sections of $PM_{2.5}$ concentrations and wind vectors."